Crystal growth, morphology and properties of NaHMP₂O₇ (M = Ni, Co, Mn, Zn, Cd, Pb)

K.Byrappa* and B.Sanjeeva Ravi Raj

Department of Geology, University of Mysore, Manasagangotri
Mysore - 570 006, India.

Abstract   Crystal growth of NaHMP₂O₇ (M=Ni, Co, Mn, Zn, Cd, Pb) has been carried out by hydrothermal technique The studies concerning the crystal growth processes and the morphology of these superionic pyrophosphates with reference to the type of cations, its ionic radii and other thermodynamic charactersitics have been carried out. Similarly the impedance spectroscopic properties of these superionic pyrophosphates have been reported

1. Introduction

Phosphates form an important group of technological materials owing to their wide range of physical and chemical properties The synthesis of phosphates began in the pervious century Superionic phosphates have been reported for the past 20 years or so Moreover, all the superionic phosphates reported soon after discovery of NASICON were all orthophosphates. For the first time our group reported high ionic conductivity in condensed phosphates, viz , pyrophosphates [1-3] Since then a lot of work is going on in this direction In the present work, the authors have studied the morphology of these crystals in great detail, with reference to the type of cation, ionic radii and thermodynamic characteristics These studies give an insight into the crystal growth of such superionic compounds in general. Also the impedance spectroscopic properties of these superionic pyrophosphates are given in brief

2. Crystal Growth

Crystal growth experiments were carried out under three different PT conditions (i) hydrothermal crystallization under lower pressure and temperature conditions; (ii) hydrothermal crystallization under moderate pressure and temperature conditions, (iii) hydrothermal crystallization under higher pressure and temperature conditions

In the first case, experiments were carried out in small autoclaves(temperature 100 - 250°C, pressure 100 - 200 bars) and smaller Morey autoclaves provided with teflon liners The starting solutions were prepared either by dissolution of P₂O₅ in water or by directly taking H₃PO₄ followed by the addition of respective carbonates or oxides or nitrates or chlorides of respective cations or by the introduction of respective hydroxide into the H₃PO₄ in various proportions (maximum filling 70%) The alkaline component of the starting materials was used in the form of a molar solution of a a definite molarity and this solution acts as a mineralizer Since the crystallization occurred by spontaneous nucleation, the temperature of the furnace was slowly increased to control the rate of nucleation The experimental temperature range was 200-300°C and the duration was 7 to 10 days The experimental conditions are given in Table 1

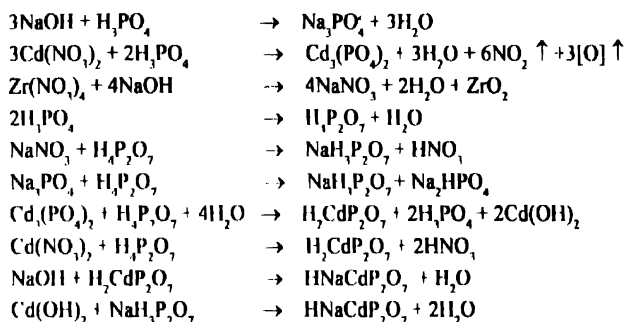*Author for correspondence E-mail BYRON@XHASIIGA VSNI. NEI IN

Table 1. Experimental conditions for low temperature hydrothermal synthesis

Compound	Nutrient (solvent)	Components & mineralizer		Temp (T°C)	Pressure (bars)	% fill	Duration (days)	Size (mm)	Colour

a) H_3PO_4 (ml), NaOH (ml), CdO (gm), $Zr(NO_3)_4$ (gm)

H_3PO_4 (ml)	NaOH (ml)	CdO (gm)	$Zr(NO_3)_4$ (gm)	Temp (T°C)	Pressure (bars)	% fill	Duration (days)	Size (mm)	Colour
i)									
4	5(5M)	1	0 5	250	80	40	8	2-3	Yellowish grey
5	5(5M)	1	0 5	250	70	30	8	2-5	Yellowish grey
6	5(5M)	1	0 5	250	80	40	8	1-3	Yellowish grey
ii)									
5	5(2M)	1	0 5	250	85	35	8	dissolved	
5	5(3M)	1	0 5	250	85	35	8	crystalline material	yellowish grey
5	5(4M)	1	0 5	250	85	35	8	1-3	Yellowish grey
5	5(5M)	1	0 5	250	85	35	8	1-4	Yellowish grey
5	5(6M)	1	0 5	250	85	35	8	1-3	Yellowish grey
5	5(7M)	1	0 5	250	85	35	8	0.5	Yellowish grey
iii)									
5	5(5M)	1	0 3	250	85	35	8	1-3	Yellowish grey
5	5(5M)	1	0 4	250	85	35	8	1-3	Yellowish grey
5	5(5M)	1	0 5	250	90	40	8	1-6	Yellowish grey
5	5(5M)	1	0 6	250	85	38	8	0.5-2	Yellowish grey
5	5(5M)	1	0 75	250	90	40	8	0.5-1	Yellowish grey
5	5(5M)	1	0 90	250	95	45	8		irregular
iv)									
5	5(5M)	0 5	0 5	250	80	32	8	1-2	Yellowish grey
5	5(5M)	0 75	0 5	250	80	32	8	1-2	Yellowish grey
5	5(5M)	1 00	0 5	250	85	35	8	2-5	Yellowish grey
5	5(5M)	1 50	0 5	250	90	40	8	1-3	Yellowish grey

b) H_3PO_4 (ml), NaOH (ml), $Co(NO_3)_4$ (gm), $Zr(NO_3)_4$ (gm)

H_3PO_4 (ml)	NaOH (ml)	$Co(NO_3)_4$ (gm)	$Zr(NO_3)_4$ (gm)	Temp (T°C)	Pressure (bars)	% fill	Duration (days)	Size (mm)	Colour
i)									
5	5(5M)	1	0 3	250	80	32	8	0 5-2	pink
5	5(5M)	1	0 4	250	85	35	8	0.5-2	pink
5	5(5M)	1	0.5	250	85	35	8	1-4	pink
5	5(5M)	1	0 6	250	85	35	8	1-3	pink
ii)									
5	5(5M)	0 5	0 5	250	85	35	8	1	pink
5	5(5M)	0 75	0 5	250	85	35	8	1-2	pink

The experiments under moderate PT conditions were carried out by using Morey autoclaves and Tuttle autoclaves within the temperature and pressure range P=150-800 bars, T=250-400°C using teflon and platinum liners respectively. In some experiments the results were much superior compared to the lower PT conditions with regard to the crystal quality and size.

The experiments under higher PT conditions were conducted using Tuttle cold-cone sealed autoclaves provided with platinum liners (T =700°C and P = 1 5 Kbars). The results of these experiments are different. The authors obtained compounds without a proton in their composition, like $NaFeP_2O_7$, $NaCoP_2O_7$ which are isostructural to allaudite.

The crystallization processes for the formation of $HNaMP_2O_7$ (where M = Ni, Co, Mn, Pb and Cd) crystals have been studied, based on solvent-solute interactions and the complexation processes is described thorough the following reaction series with regard to $HNaCdP_2O_7$:

$$3NaOH + H_3PO_4 \rightarrow Na_3PO_4 + 3H_2O$$
$$3Cd(NO_3)_2 + 2H_3PO_4 \rightarrow Cd_3(PO_4)_2 + 3H_2O + 6NO_2\uparrow + 3[O]\uparrow$$
$$Zr(NO_3)_4 + 4NaOH \rightarrow 4NaNO_3 + 2H_2O + ZrO_2$$
$$2H_3PO_4 \rightarrow H_4P_2O_7 + H_2O$$
$$NaNO_3 + H_4P_2O_7 \rightarrow NaH_3P_2O_7 + HNO_3$$
$$Na_3PO_4 + H_4P_2O_7 \rightarrow NaH_3P_2O_7 + Na_2HPO_4$$
$$Cd_3(PO_4)_2 + H_4P_2O_7 + 4H_2O \rightarrow H_2CdP_2O_7 + 2H_3PO_4 + 2Cd(OH)_2$$
$$Cd(NO_3)_2 + H_4P_2O_7 \rightarrow H_2CdP_2O_7 + 2HNO_3$$
$$NaOH + H_2CdP_2O_7 \rightarrow HNaCdP_2O_7 + H_2O$$
$$Cd(OH)_2 + NaH_3P_2O_7 \rightarrow HNaCdP_2O_7 + 2H_2O$$

The study of complexation process with reference to the solvent-solute interaction is of great importance to understand the crystallization of any compound [4] including pyrophosphates. Reports of such studies are seldom found in the literature for superionic phosphates

The crystallization process involving many chemical interactions, lead to the formation of a stable complex in the following stages (i) Acid-base interactions, (ii) Formation of metal-aqua complexes ; (iii) Interaction between acid-base and metal-aqua complexes

A series of experiments have been carried out with several divalent and trivalent metals and it was found that the divalent metals enter the composition more easily than trivalent metals. However, nutrient material show that only Al^{3+} enters the composition readily forming $Na_2H_4Al(P_2O_7)_2$ even at lower PT conditions (P < 100 bars, T =250°C), while others insist upon higher temperature of synthesis [5]

3. Morphology

A number of factors such as the degree of supersaturation, type of the solvent, pH of the mineralizer, etc affect the habit of crystal. Habit modifications occur with significant changes in the growth temperature and also with the presence of impurities in the growth media [6] The pyrophosphates show a wide range of morphological variations. The characteristic habits of

some selected pyrophosphates are shown in Figures 1(a-g) The habits exhibited by these pyrophosphates are given in Table 2 The crystal faces of most of the superionic pyrophosphates are more or less smooth and vitreous in lustre, and transparent The morphology of these pyrophosphates varies from one another depending upon the cations present.

Table 2 Morphology of pyrophosphates

Compound	System	Crystal form(s)
$Na_2H_3Al(P_2O_7)_2$	Monoclinic	Third order pinacoid side pinacoid
$HNaCoP_2O_7$	Triclinic	Third order pinacoid Second order pinacoid Fourth order pinacoid
$HNaNiP_2O_7$	Triclinic	Basal pinacoid positive and negative third order pinacoid
$HNaZnP_2O_7$	Triclinic	Basal pinacoid positive and negative
α-$HNaMnP_2O_7$	Triclinic	Second order pinacoid
$HNaCdP_2O_7$	Triclinic	Basal pinacoid positive and negative
$HNaPbP_2O_7$	Triclinic	Basal pinacoid
$NaFeP_2O_7$	Monoclinic	Side pinacoid positive and negative pinacoids
$Na_2CaMn_2P_2O_7$	Triclinic	Third order pinacoid

(X 30)

(a)

(b)

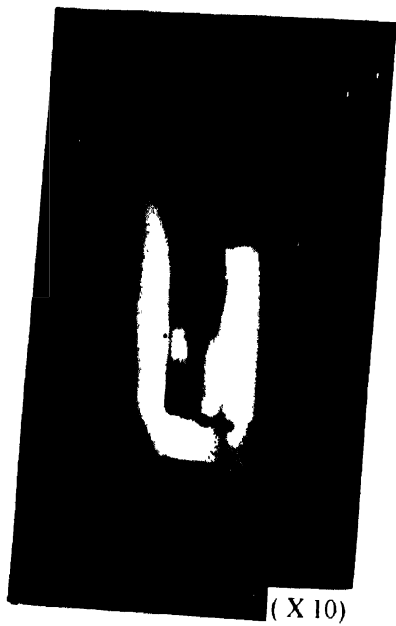(X 40)

(c)   (d)

Figure 1. Shows characteristic habits of pyrophosphate crystals (a) $H_3Na_2Al(P_2O_7)_2$; (b) α-$HNaMnP_2O_7$, (c) $HNaCoP_2O_7$ and (d) $HNaNiP_2O_7$.

Plate I(b)

(X 10)

(e)

(X 20)

(f)

(g)   (X 20)

Figure 1. Shows characteristic habits of pyrophosphate crystals · (e) HNaZnP₂O₇.
(f) HNaCdP₂O₇ and (g) HNaPbP₂O₇

Similarly, the morphology varies with respect to the degree of supersaturation, the concentration of H_2O, P_2O_5 and Na_2O in the system

It is interesting to observe that the morphology of superionic pyrophosphates vary with the variation in the cation. The cations used in the present work are Al, Mn, Co, Ni, Zn, Cd and Pb The Table 3 shows the cation properties. As evident from Table 3, the Al is the smallest ion and it show the excellent morphology (Figure la). Crystals are well developed and highly transparent   This is followed by Mn, which gives good crystals of excellent crystal habit. However, due to the susceptibility of Mn for the changes in the valency with sudden changes in the experimental growth parameters, there is a tendency for the formation of polymorphic modifications of Mn bearing superionic pyrophosphates. But both the polymorphic modifications of Mn superionic pyrophosphates show excellent morphology with well developed habit, smooth and vitreous surfaces (Figure 1b)

Table 3. Cations in superionic pyrophosphates

Element	At. No.	At. Wt.	At. radii* (Å)	Entropy at 298°K (c.u)
Al	13	65.38	1 82	6 769
Mn	25	54.93	1 79	7 59
Co	27	58.93	1 67	6 8
Ni	28	58.70	1 62	7 137
Zn	30	65.38	1 53	9 95
Cd	48	112 41	1 71	12 3
Pb	82	207 20	1 81	15 49

ref Table of periodic properties of the elements, Sargent-Welch Scientific company

The cobalt bearing superionic pyrophosphate shows probably the best morphology (Figure lc) The crystals are developed very well with vitreous, smooth and transparent surfaces. The cobalt bearing superionic pyrophosphates are bigger than the other pyrophosphates It is observed that in spite of the same crystal structure exhibited by all these pyrophosphates, they slowly lose their morphology The crystal habit in Ni is better than in Zn, because the crystals are well developed, but the crystals are mostly slender or rod shaped, transparent with smooth and vitreous surfaces (Figure Id)

In case of Zn, there is a fall in the morphological development (Figure le) like crystal habit, lustre, and transparency When we come to the Cd bearing pyrophosphate the morphological variations are still less with the crystals loosing their size, well developed habit, smooth surfaces and vitreous lustre and a low degree of transparency (Figure 1f). When the crystal surfaces were observed under higher magnification, they show more or less rough surfaces with defect structures

In case of Pb bearing surpeionic pyrophosphates, it is still worse The crystals do not have well defined crystal habit, but instead, they look more or less rounded and clustered

Table 4. Bond lengths for Superionic Pyrophosphates crystals.

Compound	Na-O (max)	Na-O (min)	Na-O Dif. (max-min)	M+1-O (max)	M+1-O (min)	M+2-O Dif. (max-min)	P1-O (max)	P1-O (min)	P1-O Dif. (max-min)	P2-O (max)	P2-O (min)	P2-O Dif. (max-min)
$Na_2AlH_3(P_2O_7)_2$	2.929	2.397	0.532	1.940	1.855	0.085	1.599	1.495	0.104	1.587	1.500	0.087
$NaMnHP_2O_7$	2.79	2.32	0.47	2.20	2.00	0.2	1.64	1.52	0.12	1.58	1.49	0.09
$NaCoHP_2O_7$	3.097	2.445	0.652	2.196	2.035	0.161	1.587	1.502	0.85	1.602	1.498	0.104
$NaNiHP_2O_7$	3.385	2.315	1.07	2.157	2.016	0.141	1.593	1.505	0.085	1.607	1.497	0.11
$NaZnHP_2O_7$	3.446	2.308	1.138	2.283	2.020	0.263	1.591	1.504	0.087	1.595	1.488	0.107

Plate II(a)

(X 100)

(a)

(X 300)

(b)

Figure 2. Shows the growth layers on (010) face of pyrophosphate crystals : (a) $HNaCoNiP_2O_7$ and (b) α-$HNaMnP_2O_7$;

Plate II(b)

(X 400)

(c)

(X 400)

(d)

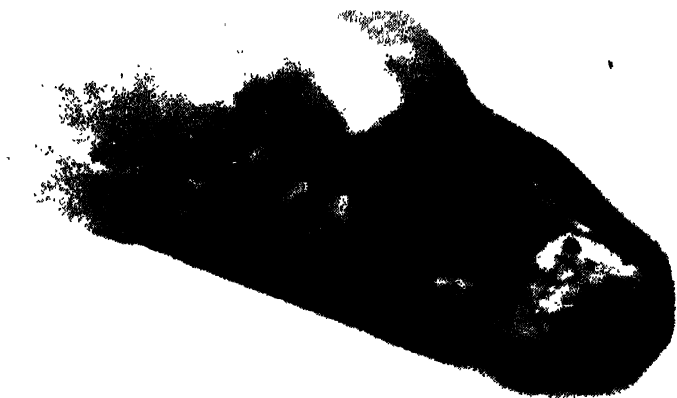**Figure 2.** Shows the growth layers on (010) face of pyrophosphate crystals : (c) $HNaZnP_2O_7$ and (d) $HNaNiP_2O_7$

Plate III(a)

(X 40)

(a)

(X 400)

(b)

Figure 3. Shows the macro steps in pyrophosphate crystals : (a) $HNaCoP_2O_7$ and (b) α-$HNaMnP_2O_7$.

Plate III(b)

(X 40)

(c)

Figure 3. Shows the macro steps in pyrophosphate crystals   (c) $HNaZnP_2O_7$.

(Figure lg). The crystals appear translucent with dull lustre and without smooth surfaces. There is a general tendency for the crystals to become polycrystalline from Mn end to the Pb end.

It is believed that all these superionic pyrophosphates belong to the same structure tyep, i.e triclinic, P_1 space group As the ionic size of the cations inserted into the structure increases, there develops a general structural distortion which in turn, affects the crystal morphology. The Table 4 shows the variation in bond lengths of these superionic pyrophosphates. As evident from the Table 4, the difference in maximum and minimum bond lengths of Na-O polyhedra increases gradually towards the Zn end member. Thus towards the Pb end member, the crystals become poorly developed The poor morphology of Cd and Pb bearing superionic pyrophosphates is due to the changes in the bond lengths and bond angles leading to the slightly higher degree of structural disorder as indicated by the preliminary X-ray single crystal diffraction studies. Also it is evident from Table 3 that the values of entropy for Zn, Cd and Pb gradually increase and these values are quite high compared to those of Mn, Al, Co or Ni Entropy is directly related to the structural disorder Thus, the thermodynamic properties of the cations also directly influence on the morphology of these new superionic pyrophosphates.

The superionic pyrophosphates show very interesting surface morphology and it varies accordingly with the growth temperature, degree of supersaturation and the cation in the nutrient. These variations also depend on the magnitude and anisotropy of the growth rates along different direction

The most commonly observed surface growth features are growth layers, grwoth steps and block structures. The surface morphology of these superionic phosphates is given in Table 5 Since these crystals belong to the lower symmetry, the effect of growth temperature, degree of supersaturation and the impurity concentration is very well depicted in their surface morphology

Table 5 Surface morphology of $HNaCoP_2O_7$ and $HNaNiP_2O_7$ crystals

Composition	Growth temp (°C)	Common faces	Growth rate	Growth features	Face
$HNaCoP_2O_7$	250	(110) (010) (1̄10)	V(101) > V(010)	Growth layers block structures	(010)
$HNaNiP_2O_7$	250	(110) (010) (011)	V(110) > V(010)	Macro steps block structures	(110)
$HNaZnP_2O_7$	250	(110) (101) (011)	V(110) > V(101)	Macro steps block structures growth layers	(101)

The Figures 2(a-d) represent the growth layers on the face (010) of the pyrophosphate crystals. Similarly Figures 3(a-c) respresent the macro steps observed in the pyrophosphate crystals As the supersaturation increased, the spirals must have become rounded. The Figure 2a shows only one half of the spirals/layers With an increase in the supersaturation and thermal oscillations, the number of macro spirals increases and a large number of thick steps appear on the surface as shown in Figure 3a The crystals obtained from experiments with surplus Na_2O

in the nutrient composition were poor in quality, may be because of the increase in the viscosity of the system And also, the crystals obtained in experiments with pH < 2 show relatively more defect features like etch pits and block structures on the as-grown surfaces of pyrophosphates crystals [Figures 4(a,b)] This corroborates the fact that pyrophosphates are stable at pH > 3 and also the high solubility of pyrophosphates in H_3PO_4.

The surface morphology of superionic pyrophosphates under investigation shows more defect structures towards the Cd and Pb end The surface morphology is well developed in the Al, Co and Ni bearing superionic pyrophosphates, as in the case of the crystal morphology. The Al, Co and Ni members show orderly arranged spirals and even a single large spiral, occasionally steps and block structures. Whereas the Cd and Pb end members mainly show block and step structures and highly discountinous surface structures. This is again connected with the highly distorted polyhedra and octahedra owing to the larger ionic radii of the transitional metals and also highly distorted polyhedra of Na-O coordination towards Cd and Pb end.

4. Characterization

The superionic pyrophosphates crystals obtained were characterised using different techinques like XRD, EPMA and impedance spectroscopy The single crystal X-ray data for the superionic pyrophosphates is given in Table 6 EPMA analysis is given in Table 7.

Table 6 X-ray data of superionic pyrophosphates

Compound	System	Space group	Cell parameters Å					
			a	b	c	β (°)	V Å^3	Z
$Na_2AlH_1(P_2O_7)_2$	Triclinic	P1̄	8 311 (4)	7 363 (4)	4.902 (3)	81 77 (2)	268 2 (4)	1
α - $HNaMnP_2O_7$	Monoclinic C_{2c}		9 935 (4)	8 455 (3)	13 106 (4)	110 75	1029 (1)	8
β - $HNaMnP_2O_7$	Triclinc	P1̄	6 657 (1)	7 372 (1)	6 517 (1)	92.22	1029	8
$HNaCoP_2O_7$	Triclinc	P1̄	6 5190(6)	6 595 (1)	6 485 (1)	92 07	255 97 (7)	2
$HNaNiP_2O_7$	Triclinc	P1̄	6 502 (3)	6 418 (1)	6.442 (2)	91 83 (1)	249 33 (7)	2
$HNaZnP_2O_7$	Triclinc	P1̄	6 509 (3)	7 250 (3)	6 486 (2)	92 09	260 37 (7)	2
$HNaCdP_2O_7$	Triclinc	P1̄	6 612	6 674	6 597	92 75	290 78	2
$NaFeP_2O_7$	Monoclinic		11 83	12 527	6 44	114 18	870 63 (2)	-

The CIS measurements were carried out using Solatron Impedance Analyser system (Model 1260) from 1 Hz to 32 MHz The pellets were made by pressing the superionic polycrystalline powder at 5 ton/cm^2 pressure The impedance data was analysed using EQUIVALENT CIR-CUIT (EQUIVCRT PAS) PROGRAM [7] The complex impedance data has been analysed to extract the bulk resistance (Rb) and hence a c conductivity (σ_b)

Plate IV

(X 100)

(a)

(X 400)

(b)
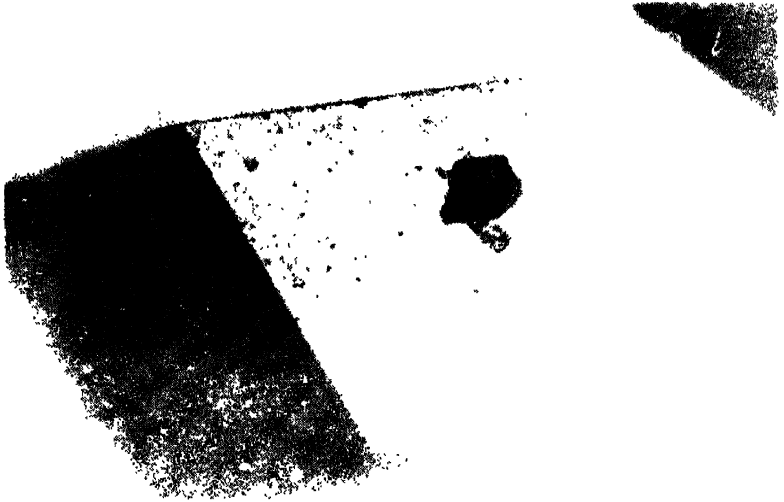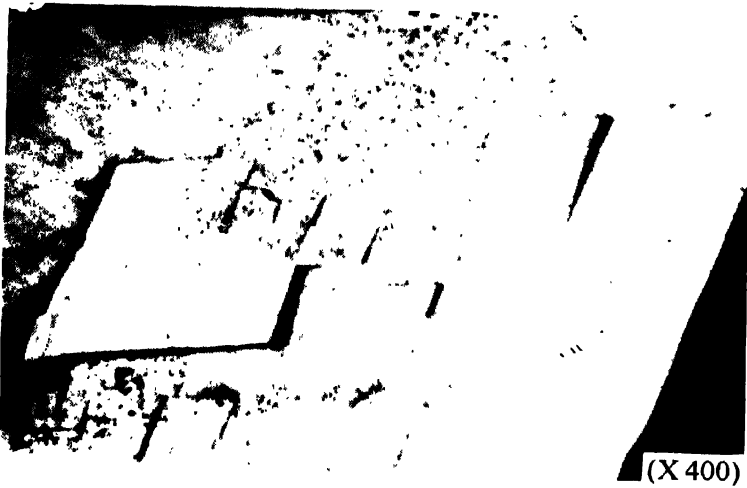
Figure 4. Shows etch pits and block structures in pyrophosphate crystals (a) $HNaCoP_2O_7$ and (b) $HNaNiP_2O_7$

The Figure 5 shows the Arrhenius plot (In $\sigma_b T$ vs 1000/T) The Arrhenius plot show single phase with an activation energy 1 1 eV for lower temperature region up to 423 K Above 423 K - 523 K, the Arrhenius plot is not linear Non-linear Arrhenius plot may be explained in terms of interfacial flicker noise due to polarization at the sample-electrode interface.

Table 7. EPMA analysis of superionic pyrophosphates

Oxide	HNaCoP$_2$O$_7$ Wt%	HNaNiP$_2$O$_7$ Wt%	HNaZnP$_2$O$_7$ Wt%	HNaMnP$_2$O$_7$ Wt%
Na$_2$O	09.92	11.67	11.42	11.17
CoO	30.67	00.10	00.10	00.00
ZnO$_2$	00.00	00.00	00.00	00.00
P$_2$O$_5$	59.45	58.18	57.94	57.46
NiO	00.04	31 11	00.00	00.00
ZnO	00.00	00.00	31.63	00.00
MnO	00.12	00.25	00.21	32.31
CaO	00.04	00.00	00 00	00.00
FeO	00.04	00 22	00.04	00.04
TiO$_2$	00.07	00.02	00.01	00.01
Total	100 35	101 56	101 25	99.99
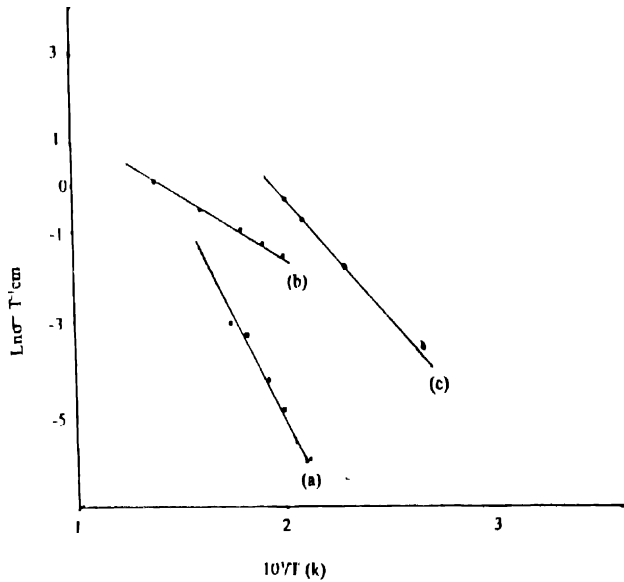
Figure 5 Arrhenius plot for pyrophosphates

References

[1] S Gali,K Byrappa and G S Gopalkrishna*Acta Cryst.*,**C45** 1667 (1989)

[2] K Byrappa,G S Gopalkrishna and S.Gali,*Indian.J.Phy.*,**63A** 321 (1989)

[3] S Gali and K Byrappa*Acta Cryst.*, **C46** (1990)

[4] K Burger *Solvation, Ionic and Complex Formation Reaction in Non-Aqueous Solvents* (Budapest   Academial Kiaddo) **42** (1983)

[5] K Byrappa *Indian J. Phys* **66A** 233 (1992)

[6] R Kern in *Growth of Crystals* **vol 8** ed. N.N. Sheftal (New York : Consultants Bureau (1969)

[7] B A Boukamp *Equivalent Circuit : Users Manual* (University of Twente, The Netherlands) (May 1989)